

Chapter 5 Multiphase Pore Fluid Distribution

Reading assignment: Chapter 3 in L. W. Lake, Enhanced Oil Recovery.

So far we have discussed rock properties without regard to the fluid other than that it was a single phase. When multiple phases exist in a rock or soil we need to be concerned about how the fluids are distributed in the pore space and how they will interfere (or assist) with the flow of when more than one phase exist. The first thing that we will see is each (immiscible) fluid has a pressure that is distinct from that of the other fluid(s) because of the curvature of the interfaces. This difference in pressure is called the **capillary pressure** and is usually shown as a function of the saturation of one of the phases. The interference in the flow is represented by the **relative permeability** and is usually shown as a function of saturation. The relative permeability of a phase has contributions to flow only from the fraction of that phase that is connected. The disconnected saturation of a phase is called the **trapped saturation**. The saturation at where the relative permeability goes to zero is called the **residual saturation** and is usually equal to the trapped saturation for a nonwetting phase.

Capillarity

Surface and interfacial tension

We know from our own experience that the pressure inside a balloon is greater than the pressure outside. We attribute the difference in pressure to the tension of the stretched rubber sheet. In the case of a rubber sheet, the tension is a function of how much it has been stretched from some equilibrium shape. There is also a tension between two immiscible fluid phases. The origin of the tension between immiscible phases is due to the dissimilarity of the intermolecular forces between the molecules comprising the phases. Molecules (of nonsurfactive material) have lower net energy when it is surrounded by its own kind rather than when it is at an interface and mingling with the molecules of the other phase. Thus the tendency of molecules to leave the interface and move to the interior of the phase creates a force tending to contract the interface to a smaller area. This creates a tension that is dependent only on the presence of the interface and not on any history of how much it had been stretched. Alternatively, the interfacial region has an excess energy per unit area and the fluids will spontaneously try to reduce the interfacial area if it is not constrained. It is because of these two alternative views that the surface tension and interfacial tension have been expressed as either *dyne/cm*, a tension per unit length, or *erg/cm²*, an energy per unit area. Since an erg has the same units as dyne-cm it is easy to see that these are equivalent. The choice of units in the SI units is *mN/m* or *mJ/m²*, both equivalent to each other and to the cgs units. The tension is called **surface tension** when one phase is a gas or vapor phase. When both phases are liquid it is called **interfacial tension**. The concept of

surface energy also applies to a solid-fluid interface but in this case it is called **surface energy**.

Young - Laplace Equation

The relation between the pressure difference across an interface and tension can be determined by displacing the interface an infinitesimal distance in the direction of the normal to the interface. When the system is in mechanical equilibrium, the work to stretch (or contract) the interface is balanced by the pressure - volume work done in displacing the interface. The equation for mechanical equilibrium across a fluid interface is the Young - Laplace equation.

$$\Delta p = 2H\sigma$$

where σ is the surface or interfacial tension, H is the mean curvature, and Δp is the pressure difference across the interface such that the higher pressure is on the concave side of the interface. The mean curvature is the average of the principal curvatures (Aris 1962) or it can be expressed as a function of the radius of curvatures.

$$H = \frac{1}{2}(\kappa_1 + \kappa_2)$$

$$= \frac{1}{2}\left(\frac{1}{r_1} + \frac{1}{r_2}\right)$$

Substituting into the Young - Laplace equation, we have:

$$\Delta p = \sigma\left(\frac{1}{r_1} + \frac{1}{r_2}\right)$$

$$= P_c$$

Pressure drop in some capillary systems

We will be able to understand capillary phenomena in porous media much better if we see how the capillary pressure changes in some elementary geometry. In the following, we will consider one fluid to be wetting and the other fluid nonwetting. Also the first two systems will be axial-symmetric so the two radii of curvature are equal. Consider first Fig. 5.1 where a nonwetting fluids enters a circular pore from a bulk reservoir. The capillary pressure will increase with volume until it reaches a limiting value of $2\sigma/R$.

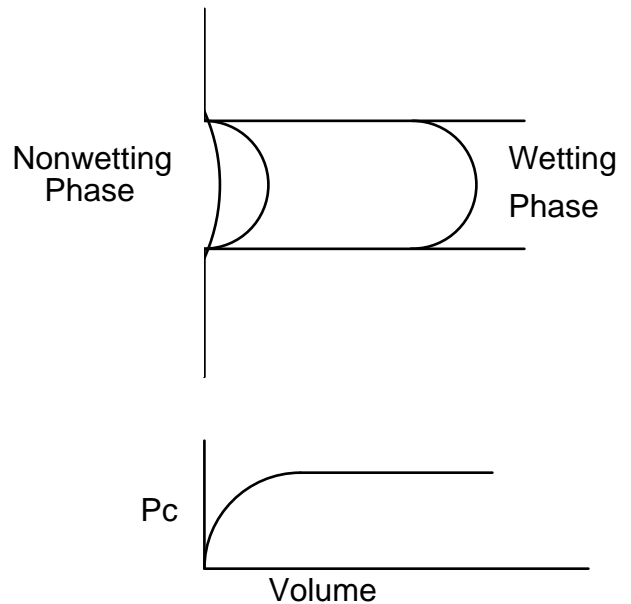


Fig. 5.1 Nonwetting fluid entering pore

Another example is a nonwetting fluid exiting a circular pore and entering a large reservoir filled with the wetting fluid as in Fig. 5.2. This is similar to blowing bubbles from a glass straw. Suppose the interface is flat at the exit of the pore after the previous bubble detached. If the non wetting phase is pumped with a controlled volumetric rate, the pressure will first increase as the interface increases in a curvature from zero (flat) to that of a hemisphere. The pressure will then decrease as the interface expands into a surface of a growing sphere. If the nonwetting fluid was a reservoir with an increasing pressure rather than at a constant volumetric rate, the bubble (or drop) will first grow slowly corresponding to the rate of pressure increase until it reaches the maximum pressure upon reaching the hemispherical shape and then it will suddenly grow in size.

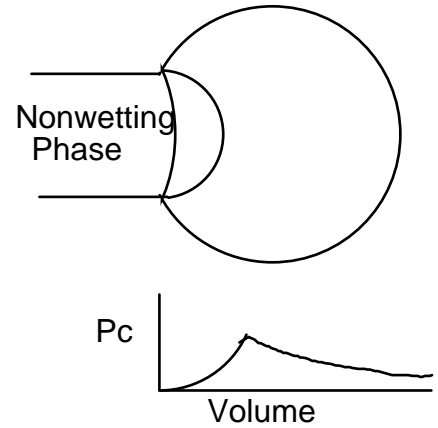


Fig. 5.2 Nonwetting fluid exiting pore

Now consider a square capillary into which a nonwetting phase has entered. The capillary pressure at which the nonwetting fluid first enters the square capillary is approximately

$$P_{ce} = \frac{2\sigma}{w/2} = \frac{4\sigma}{w}$$

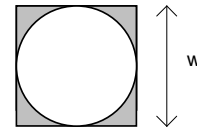


Fig. 5.3

As the capillary pressure increases above this value, the wetting phase (shaded) will be pushed further into the corners as the radius of curvature of the interface decreases. (When the nonwetting phase enters at the above capillary pressure, the wetting phase will already be pushed into the corners compared to Fig. 5.3.) Suppose now the wetting phase is allowed to flow back along the corners without the end of the drop exiting the capillary. If the capillary pressure is now then decreased below P_{CSO} , the capillary pressure of a cylindrical filament that just touches the capillary walls,

$$P_{cso} = \frac{2\sigma}{w}$$

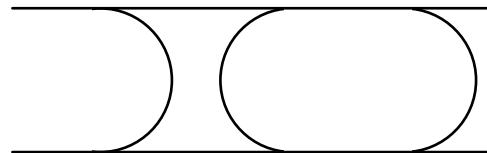


Fig. 5.4 Side view after snap-off

the interface will pull away from the walls of the capillary. The nonwetting phase is now a thin filament that is unsupported by the walls. This configuration is unstable and the nonwetting phase will neck down in some places and will swell in other places until it is supported by the walls of the capillary. The necking down is

unstable and the nonwetting phase will **snap-off** into droplets or bubbles of disconnected nonwetting phase.

Nonwetting phase trapping

Suppose the porous medium is made up of pore bodies and pore necks of many different sizes as shown in Fig. 5.5. The medium is initially saturated with the wetting phase. The nonwetting phase is first allowed to enter only the largest pores as in 5.5a and then the capillary pressure reduced to zero. Nonwetting phase will be trapped as in 5.5b. With additional cycles with increasing initial nonwetting saturation additional trapping will occur as in 5.5d and 5.5f. Such an experiment with increasing initial saturation of the nonwetting phase measuring the residual saturation at each initial saturation generates an **initial - residual saturation curve** as in Fig. 5.6. This curve probes the volume of nonwetting phase trapping sites as a function of entering increasingly finer pores. This curve can be used to determine the saturation of nonwetting phase that is trapped at a given saturation if information is available on the maximum nonwetting saturation attained, i.e., memory of its history is available.

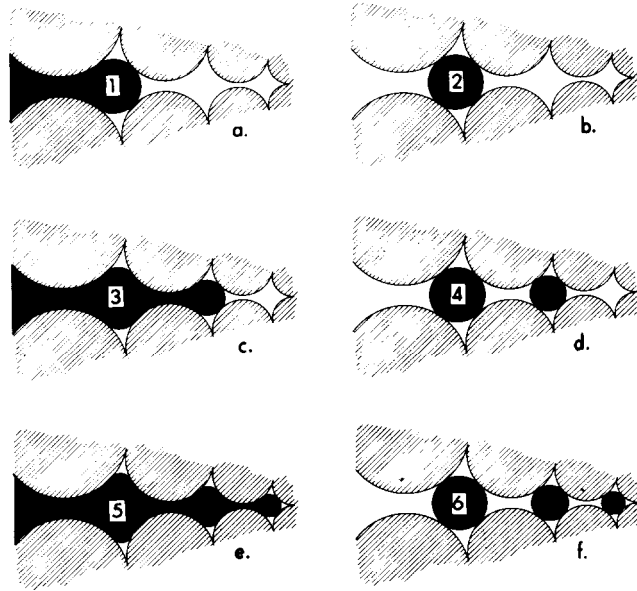


FIG. 6 PORE NETWORK CROSSECTION
NORMAL TO DIRECTION OF FLOW

Fig 5.5 Trapping in initial - residual saturation cycles (Stegemeier 1977)

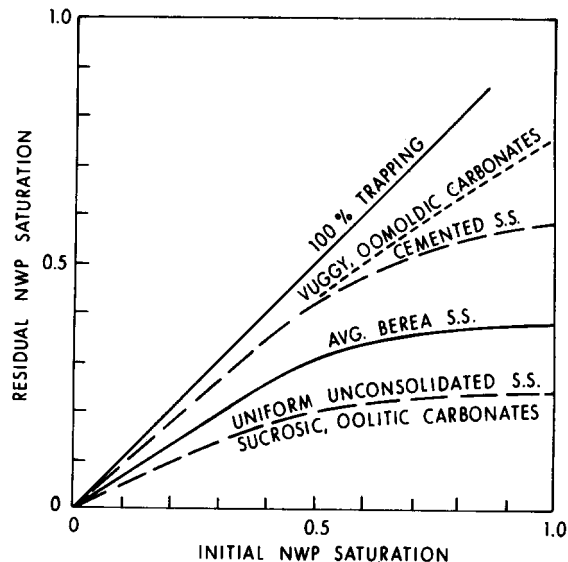


Fig. 5.6 Typical nonwetting phase trapping characteristics of some reservoir rocks (Stegemeier 1977)

Hysteresis

The initial-residual saturation curve shown in the previous section are usually measured by toluene-air counter-current imbibition or mercury-air measurements. The toluene-air measurements are more economical and are not destructive. With this method the cleaned, dry rock is initially saturated with toluene. The initial air (nonwetting phase) saturation is established by allowing the sample to dry to a measured weight. The sample is immersed in toluene and sufficient time is allowed for toluene to spontaneously imbibe into the sample (but not so long that air diffuses out of the sample). The residual air saturation is determined by weighing. This cycle is repeated for increasing initial air saturation.

The initial-residual saturation curve can also be measured when measuring the mercury - air capillary pressure curve. Fig. 5.7 illustrates a typical capillary pressure hysteresis curve measured in the course of measuring the initial-residual curve. This figure shows that the capillary pressure curve is not a unique function of saturation. The capillary pressure curve is a function of the saturation history. During primary drainage, nonwetting phase has not entered pores with a pore throat smaller than the current value of the capillary pressure. However, if the sample had attained a higher mercury saturation previously in its history, then there will be some trapped nonwetting phase in the smaller pore network. Thus, the nonwetting phase saturation is higher at the same capillary pressure by the amount equal to the trapped nonwetting phase in the smaller pore network. For example, compare curves 1, 3, and 5 in Fig. 5.7. A practical way to account for the hysteresis is to store a memory of the maximum nonwetting phase attained. The residual saturation is a function of this maximum initial saturation as determined from the initial-residual curve. The capillary pressure and relative permeability functions (to be introduced later) will be normalized to go to zero at this value of residual saturation.

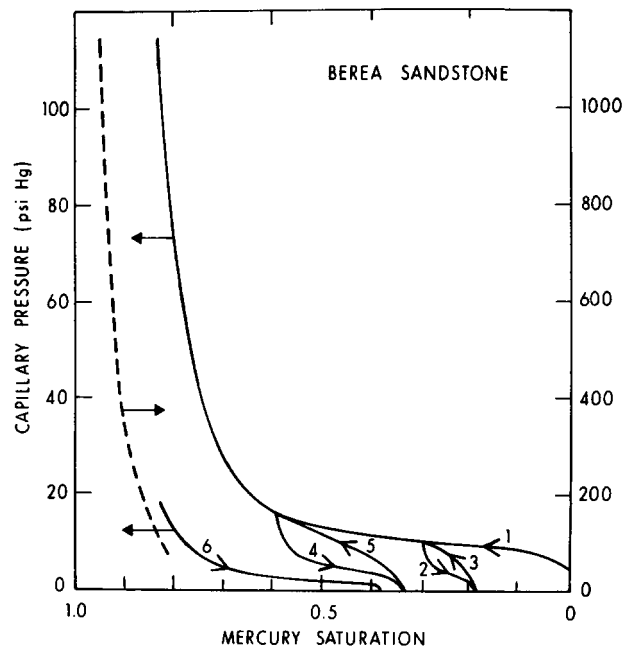


Fig. 5.7 Capillary pressure initial-residual hysteresis curves (Stegemeier 1977)

Capillary Desaturation

Earlier we discussed trapping of a nonwetting phase under near static conditions. We may ask the question, "Would the amount trapped be the same under dynamic conditions?" or "If we apply a large enough pressure gradient or buoyancy force, can a trapped nonwetting phase be remobilized?" and "For a given pressure gradient, will the amount trapped and remobilized be the same?"

First lets look at the shape of a trapped nonwetting phase to ask what will it take to mobilize the "blob". Fig. 5.8 illustrates such a blob that spans a few pore bodies. Suppose that there is a pressure gradient that is trying to displace the blob from left to right. The blob is being stopped from moving because the front of the blob must squeeze through a pore throat. Lets say that the pore throat radius is r_n . The capillary pressure at the front of the blob must exceed the capillary entry pressure of that pore throat for the blob to pass through. i.e.,

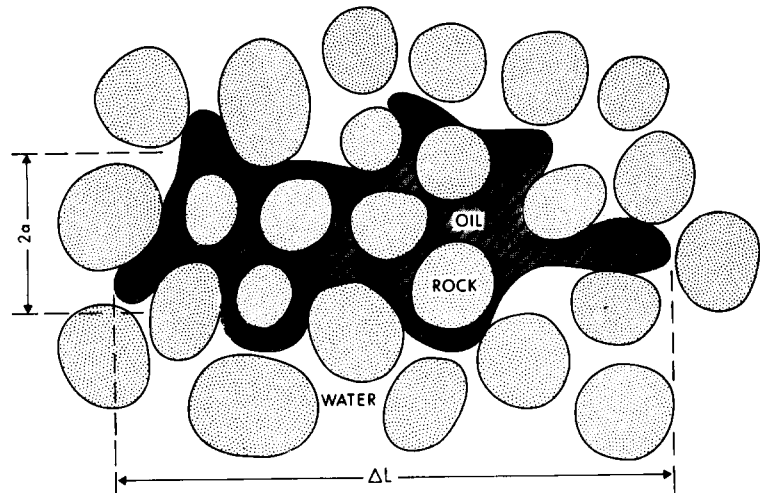


Fig 5.8 Schematic of trapped oil "blob" (Stegemeier 1977)

blob must exceed the capillary entry pressure of that pore throat for the blob to pass through. i.e.,

$$P_{c,front} \geq \frac{2\sigma}{r_n}$$

Suppose that the back of the blob that is a distance L away from the front is flattened by the pressure gradient. The capillary pressure at the back of the blob is then equal to zero. The pressure gradient within a static blob is zero. The pressure gradient in the wetting phase is that due the flow of the wetting phase and is given by Darcy's law. The pressure drop in the wetting phase over the distance L is

$$\Delta p = \frac{u_w \mu_w}{k_w} L$$

Since this is the pressure drop across the length of the blob and the capillary pressure at the back of the blob is zero, this must be equal to the capillary pressure at the front of the blob. The criteria for mobilizing the blob is now

$$\frac{u_w \mu_w}{k_w} L \geq \frac{2\sigma}{r_n}$$

Lets express the length of the blob and the permeability in terms of the pore throat radius.

$$L = \alpha r_n$$

$$k_w = \beta r_n^2$$

Substituting into the criterion for mobilizing the blob, we have

$$\frac{u_w \mu_w}{\sigma} \geq \frac{\beta}{\alpha}$$

The right side is the ratio of dimensionless quantities and the left side is a well known dimensionless number called the **capillary number** or viscous to capillary ratio.

$$N_{vc} = \frac{u\mu}{\sigma}$$

If the driving force for displacement was buoyancy rather than the pressure gradient, the dimensionless number would be the Bond number. Combination of both these driving forces results in the Brownell Katz number. The B-K number and capillary number differ by a numerical factor equal to the water relative permeability at the residual nonwetting phase saturation. The above is a very condensed discussion of oil entrapment and mobilization. For a through discussion see the reviews by Stegemeier (1977), and Lake (1989).

The capillary number criterion groups the easily measured parameters. It does not have parameters for the variability of the pore structure of the rock. Thus one would expect desaturation to occur over a range of capillary numbers and this range would be different for different rocks. Fig. 5.9 has some measured capillary desaturation data measured by different investigators. Fig. 5.10 shows similar data except that $1/\lambda_{rt}$ is used instead of μ . The difference between these is the relative permeability to water at the residual oil saturation. Fig. 5.10 using this definition for the capillary number, show the same correlation can be applied for the wetting phase with a small offset. However, there is a conceptual difference with the "trapping" of a wetting phase. The wetting phase remains continuous rather than as a "blob" when it approaches being immobile. The length of the wetting phase "blob" is thus equal to the length of the rock sample and thus the sample length should be a parameter in the residual wetting phase saturation.

It may be difficult to increase the pressure gradient over several orders of magnitude to displace residual oil. However, with surfactants the oil-water interfacial tension can be reduced from 30 mN/m to 10^{-3} mN/m. Thus the surfactant flooding enhanced oil recovery (EOR) process.

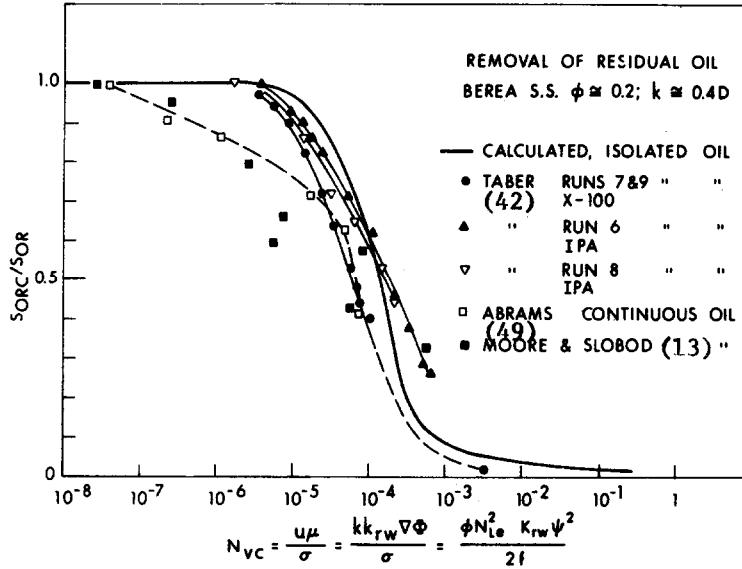


Fig. 5.9 Capillary desaturation curves; the curve by Abrams apply to dynamic trapping, the other curves apply to mobilization of trapped oil (Stegemeier 1977)

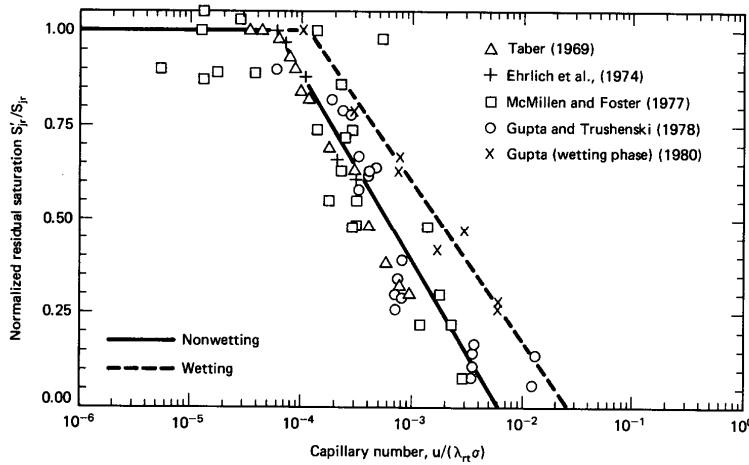


Fig. 5.10 Capillary desaturation expressed in terms of the relative total mobility rather than water viscosity [Lake 1989 (Camilleri 1983)]

Relative Permeability Models

Normalized Saturation for Relative Permeability and Capillary Pressure

We saw how the residual saturation can differ because of the saturation history or the capillary number. The relative permeability and capillary pressure curves will change as the residual oil saturation is changed. A commonly used approach is to express the relative permeability and capillary pressure as a function of the normalized saturation.

$$S = \frac{(S_w - S_{wi})}{(1 - S_{or} - S_{wi})}$$

The power law model for relative permeability is

$$k_{rw} = k_{rw}^o S^{n_w}$$
$$k_{ro} = k_{ro}^o (1 - S)^{n_o}$$

where the coefficient is the end point relative permeability when the other phase is at the residual value and the exponent is commonly called the Corey exponent. It is approximately equal to 4.0 for the wetting phase and 2.0 for the nonwetting phase. Additional models will be discussed later.

Assignment 5.1 Plots of relative permeability

Plot oil and water relative permeability versus water saturation with linear and log scale for the relative permeability. Use the following parameters:

Parameter	Value
S_{wi}	0.25
S_{or}	0.25
k_{ro}^o	1.0
k_{rw}^o	0.15
n_w	4.0
n_o	2.0

Original Model of Corey

The power law model presented earlier is often called the "Corey model" even though it is not the same as the model originally presented by A. T. Corey in 1954. A number of investigators prior to that time had been attempting to correlate the relative permeability curves with the pore size distribution determined from the capillary pressure curves and a saturation dependent

tortuosity function. For example, the equation used by Burdine appears as follows:

$$k_{ro} = \left(\frac{S_o - S_{or}}{1 - S_{or}} \right)^2 \frac{\int_0^{S_o} dS'_o / P_c^2}{\int_0^1 dS'_o / P_c^2}$$

$$k_{rg} = \left[1 - \left(\frac{S_o - S_{or}}{S_m - S_{or}} \right) \right]^2 \frac{\int_{S_o}^1 dS'_o / P_c^2}{\int_0^1 dS'_o / P_c^2}$$

where

S_o is the oil (wetting phase) saturation

S_{or} is the residual oil (wetting phase) saturation

S_m is the lowest oil (wetting phase) saturation at which the gas (nonwetting phase) tortuosity is infinite, i.e., $1 - S_{gr}$ or $1 -$ residual nonwetting phase

Corey sought to measure gas (nonwetting phase) relative permeability and estimate the oil (wetting phase) relative permeability. He observed that $1/P_c^2$ could be approximated as proportional to $S_o - S_{or}$ for $S_o > S_{or}$ for the high permeability rocks he was examining. His resulting equations for the oil and gas relative permeabilities are as follows:

$$k_{ro} = \left(\frac{S_o - S_{or}}{1 - S_{or}} \right)^4$$

$$k_{rg} = \left[1 - \left(\frac{S_o - S_{or}}{S_m - S_{or}} \right) \right]^2 \left[1 - \left(\frac{S_o - S_{or}}{1 - S_{or}} \right)^2 \right]$$

These equations have two parameters, S_{or} and S_m . Keep in mind that oil is the wetting phase in a oil-gas system.

Fig. 5.11 compares his measured and calculated oil (wetting phase) relative permeabilities. These results show that the wetting phase relative permeability can be modeled with the power law model with the exponent equal to 4.0 and an initial 100% wetting phase saturation where the end point relative permeability is equal to 1.0. Corey was not attempting to verify his model of the gas (nonwetting phase) relative permeability. However, if you compare his k_{rg} equation with the power law model, it appears like the power law model with an exponent equal to 2.0 and another factor that is close to unity except for high wetting phase saturation. The power law model is commonly called the "Corey model" with the exponents as estimated parameters. Notice that in Fig. 5.11 the value of S_{or} is 0.28 but yet the curve appears to go to zero at a liquid saturation of 0.45. When relative permeability is plotted on a linear scale, the small values of relative permeability become indistinguishable from zero. The relative permeability should be plotted on a logarithmic scale to examine the small values of relative permeability. Fig. 5.12 shows a curve plotted on a logarithmic scale. The part of the curve below 0.01 would have been indistinguishable from zero on a linear plot.

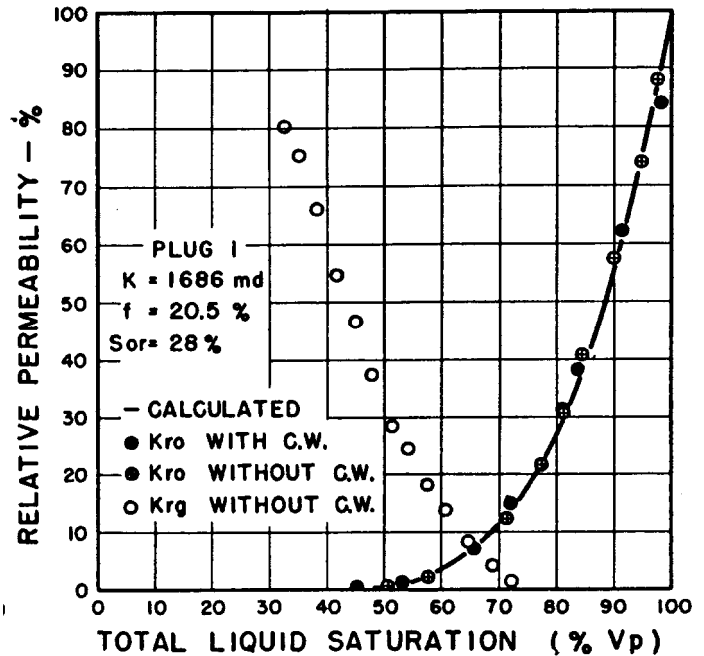


Fig. 5.11 Relative permeabilities for consolidated sand (Corey 1954)

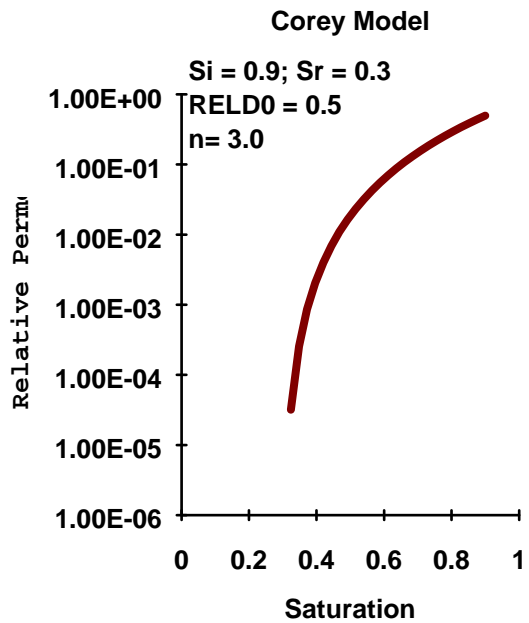


Fig. 5.12 Appearance of relative permeability with logarithmic scale

Nonwetting Model

The power law model differs slightly from the original nonwetting phase relative permeability model of Corey. When the pore size distribution is very wide (such as when a significant amount of clays are present), the nonwetting phase relative permeability does not change much with increasing wetting phase saturation at small wetting phase saturation. The wetting phase is occupying the smaller pores which contributed little to the permeability of the nonwetting phase. In this case, the nonwetting phase relative permeability is S shaped on a linear plot. Proper description of the shape of the oil (or gas) relative permeability curve at high oil (or gas) saturation is important in the calculation of the original productivity of wells that are in the capillary transition zone. The shape of the curve for high nonwetting phase saturation can be modified from the power law model to fit the S shaped part of the curve as follows.

Suppose that below some nonwetting phase saturation, S_x , the relative permeability can be described by the power law model or Corey model. At high nonwetting phase saturation, the reduction of the nonwetting phase relative permeability should be approximately equal to the wetting phase relative permeability. Corey has shown that the wetting phase relative permeability can be described by the power law model. Thus we should expect the reduction in the nonwetting phase relative permeability at high nonwetting phase saturation to approach the reduced wetting phase saturation raised to an exponent. The types of behavior below and above S_x should blend together with no discontinuity in the slope of the relative permeability. A model that meets these requirements is as follows.

$$k_{r_{nw}}(S_{nw}) = k_{r_{nw}}^o \left[1.0 - (1.0 - S)^{m(S)} \right]^{n(S)}$$

where

$$S = \frac{(S_{nw} - S_{nwr})}{(S_{nwi} - S_{nwr})}$$

$$SS = \frac{(S_x - S_{nwr})}{(S_{nwi} - S_{nwr})}$$

IF($S < SS$) THEN

$$n(S) = n_o$$

$$m(S) = 1.0$$

ELSE

$$n(S) = n_o - (n_o - 1.0) \left(\frac{S - SS}{1.0 - SS} \right)^2$$

$$m(S) = 1.0 + (m_o - 1.0) \left(\frac{S - SS}{1.0 - SS} \right)^2$$

ENDIF

where

S_x nonwetting saturation where the models change
 m_o exponent for wetting phase (adjustable parameter)
 n_o Corey exponent for nonwetting phase below S_x

The following figures illustrate the nonwetting phase relative permeability model.

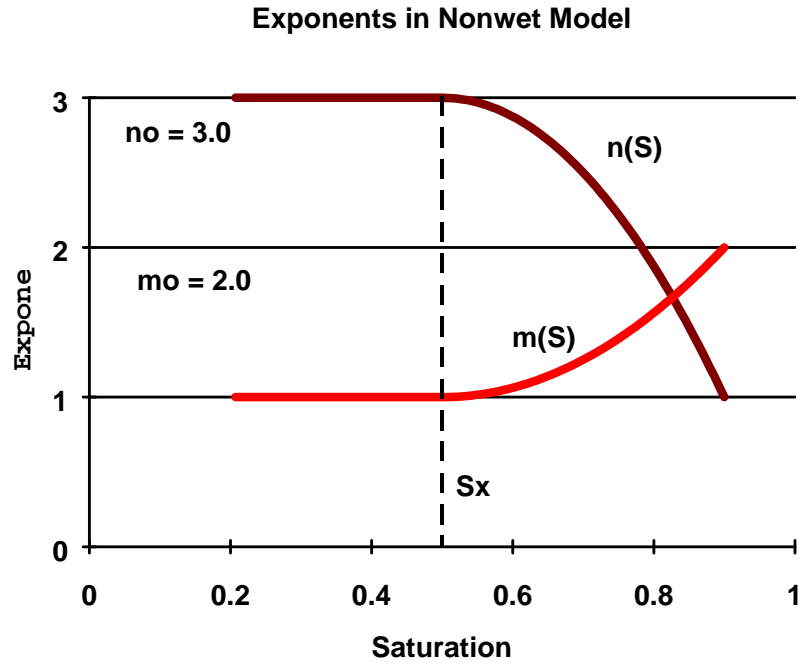


Fig. 5.13 Exponents for the nonwet relative permeability model

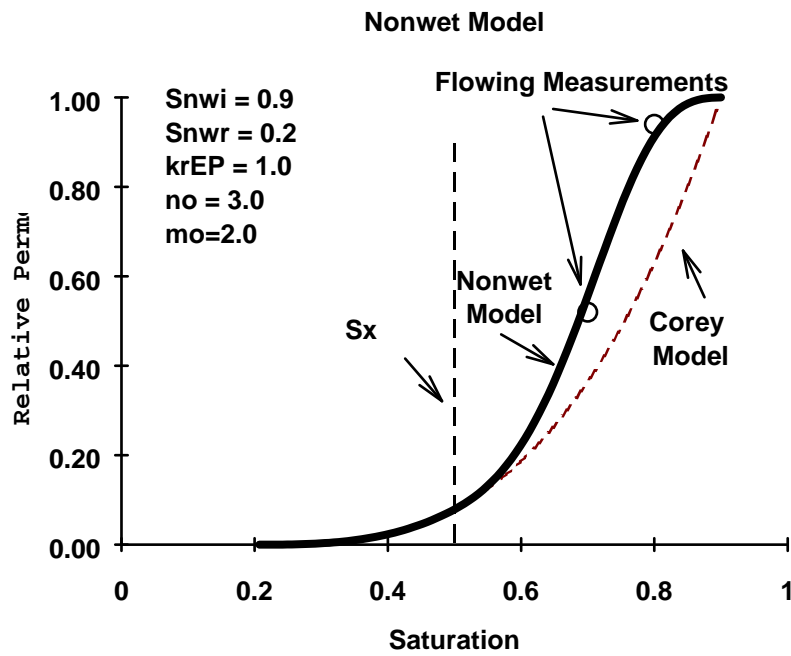


Fig. 5.14 Nonwet relative permeability model

Effect of Wettability

So far we have assumed that the systems are water-wet. This is generally the case with clean sandstone and refined oil. However, crude oils have surface active components that have varying degree of tendency to adsorb on the mineral surfaces cause the crude oil to adhere to the pore walls. An extreme case of reversal of wettability from water-wet to oil-wet is illustrated in Fig. 5.15. The wetting phase occupy the smaller pores and thus have a smaller relative permeability for the same saturation. Also, if the Corey exponents were calculated, a larger Corey exponent would be expected for the wetting phase.

Systems with crude oil have varying degrees of wettability. Fig. 5.16 illustrates the remaining oil saturation in a core as a function of the wetting index and pore volumes of water throughput. The wettability index is -1.0 for oil-wet and $+1.0$ for water-wet conditions. When the system is water-wet the oil is trapped by the snap-off mechanism. The oil production stops abruptly soon after water breakthrough. When the system is oil-wet the remaining oil is in the smaller pores which make a small contribution to the relative permeability for a given saturation. The oil production tails out over many pore volumes of throughput because the oil relative permeability is small but nonzero. When the system is intermediate in wetting index, snap-off is inhibited and the oil is less likely to be in the smaller pores and thus less oil remains after waterflooding.

Absolute and End Point Permeability

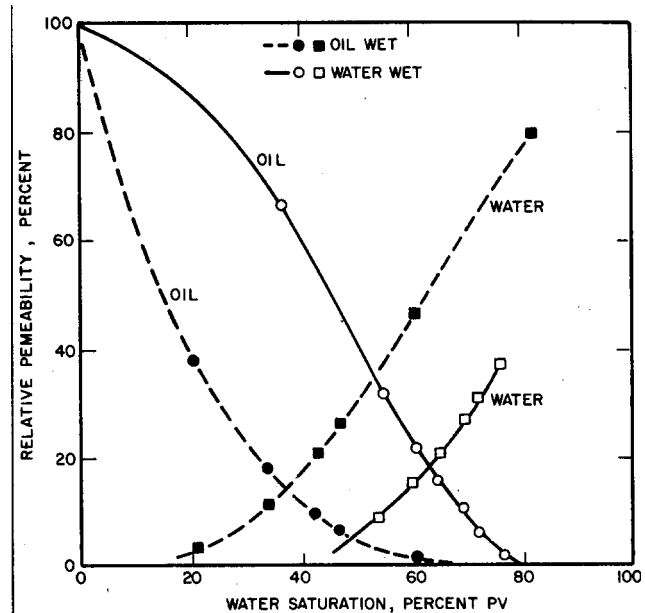


Fig. 5.15 Steady state relative permeability with heptane and brine in alundum core. The oil wet core was treated with organochlorosilanes (Lennings 1957)

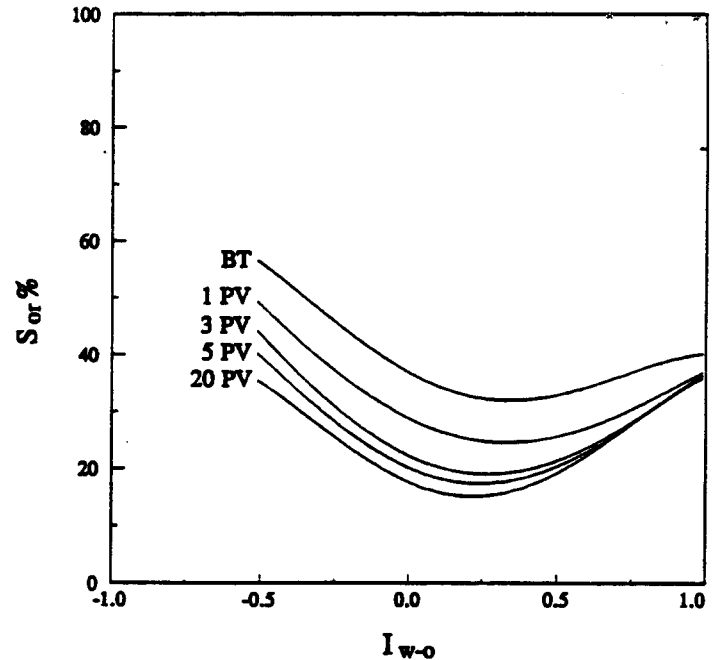


Fig. 5.16 Remaining oil saturation after waterflooding (Jadhunandan and Morrow, 1991)

Relative permeability is formally defined as the ratio of the permeability to a phase divided by the absolute permeability. Absolute permeability is defined as the permeability to a single phase. In the absence of clays, the single phase permeability measured with brine, refined oil, or gas (properly extrapolated to infinite pressure) should not differ. However, in practice the brine permeability is usually less than the single phase permeability to air or refined oil because the clays collapse in the absence of an aqueous phase.

Many companies normalize the relative permeability with respect to the oil permeability at the initial oil saturation (i.e., at "connate" water saturation). This will result in the end point relative permeability for oil being identically equal to 1.0. People who use this definition of relative permeability argue that this normalizes the oil permeability with respect to the conditions of the reservoir before waterflooding. However, this creates difficulties when comparing relative permeabilities as a function of different initial oil saturation or different wettability because both will cause a change in the permeability to oil at initial saturation even though the absolute permeability is not changing. For example, suppose the relative permeability are measured with different initial oil saturation. If the relative permeabilities are normalized with respect to the oil permeability at initial saturation, then the water relative permeability curves will appear to change with different initial oil saturation.

Three Phase Relative Permeability

Three phase relative permeability measurements and models have given widely different results since the 1950's. It is generally accepted that in water-wet systems, the water (wetting phase) and gas (nonwetting phase) can be expressed as a function of their own saturation. However, the oil phase is the nonwetting phase in a water-oil system and is the wetting phase of a gas-oil system in the presence of connate (or irreducible) water saturation. The literature has numerous models to estimate three phase oil relative permeability from water-oil and gas-oil (at connate water) curves. A recent survey of the models by Baker lead him conclude that "there are many problems remaining to be solved" and recommended that the three phase oil relative permeability be calculated by straight line interpolation between the water-oil and gas-oil at connate water data. The resulting oil isoperm contours will look as in Fig. 5.17.

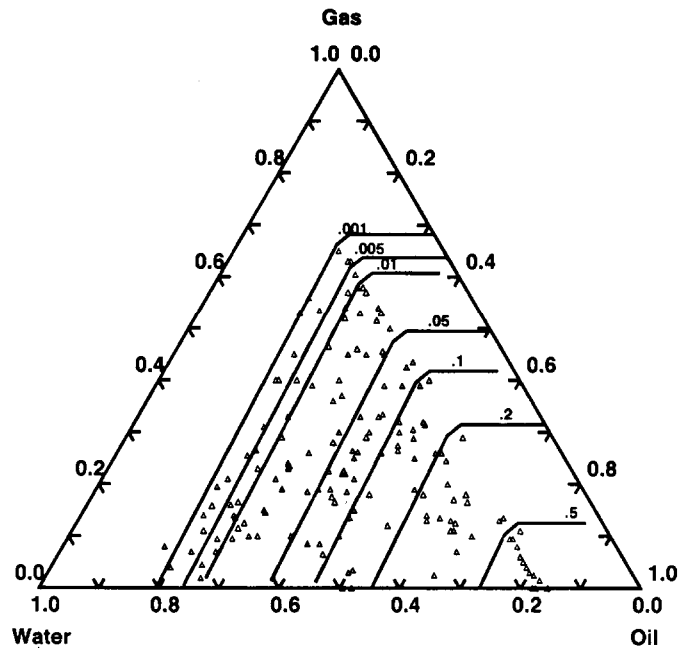


Fig. 5.17 Three phase oil isoperms using linear interpolation of the two phase data (Baker 1988)

Measurement Methods

Measurement

Unsteady State Method The unsteady state method is the classic method used to measure relative permeability. The core sample at a uniform initial oil is water flooded (or gas flooded) while the oil and water (or gas) production and the pressure drop across the core is monitored. This method is based on the Buckley-Leverett theory of two phase displacement, the Welge method to estimate outflow end saturation from the cumulative production, and the Johnson, Bossler, Neumann method to obtain individual relative permeability rather than the ratio by using the pressure information.

An advantage of the unsteady state method is that it is rapid and the apparatus is simple. Disadvantages are that: (1) flow may not be one dimensional due to viscous fingering or gravity segregation, (2) if the mobility ratio is favorable, then much of the saturation may be in the shock region from which no relative permeability information can be obtained, and (3) hold up of the wetting phase at the outflow end tends to retard the flow of the wetting phase by capillary pressure effects.

Steady State Method The steady state method gives the most accurate measurement of relative permeability. The only disadvantage of a properly designed equipment and technique is that the equipment is complex and the

measurements are time consuming. An early steady state apparatus is illustrated in Fig. 5.18. Water and oil (or gas and oil or three phases) are injected at controlled ratio and measurements of pressure drop and saturation are made when steady state is reached. Advances in technology have been made in measurements of saturation. Current methods include X-ray CT scanning, X-ray or gamma ray attenuation and recycling of the fluids. The end section serves to displace the capillary end effect mentioned earlier beyond the test section. The test section can include several core plug samples butted together to increase the length of the test section. A combined method uses the steady state method for all water/oil ratios and a unsteady state interpretation for the final, 100% water injection.

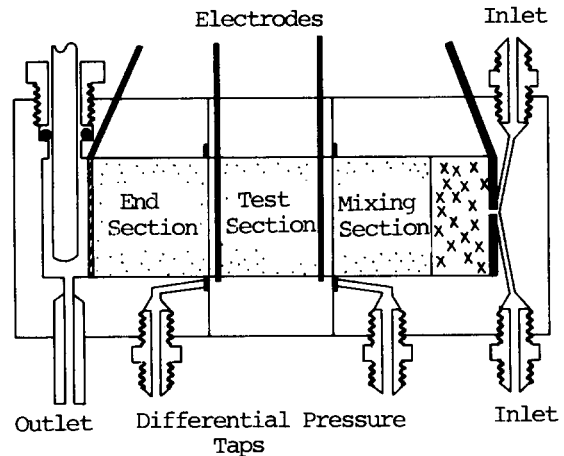


Fig. 5.18 Steady state apparatus with electrical resistivity measurements to estimate saturation [Honarpour, Koederitz, Harvey 1986 (Geffen, et al 1951)]

Centrifuge Measurements

Fig. 5.19 illustrates an early automated centrifuge for measuring relative permeability and centrifuge. The method used centrifugal acceleration and buoyancy as the driving force for displacement. The core holder can be arranged so that either the more dense or the less dense fluid is the displaced phase. Recent (Hirasaki et al 1992) improvements include improved electronics to measure speed and production at rates up to 10 Hz to interpret the early production. The interpretation software now includes the effects of the mobility of the invading phase and the effects of capillary pressure.

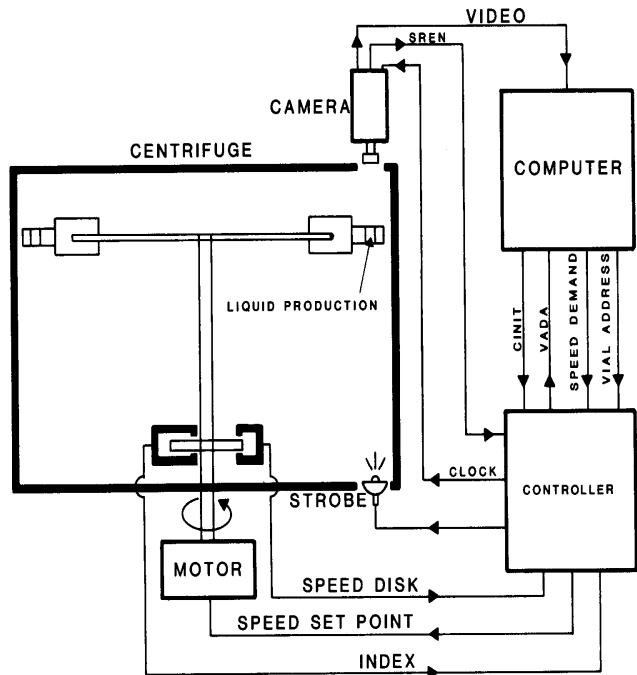


Fig. 5.19 Illustration of early centrifuge relative permeability and capillary pressure device [Honarpour et al 1986 (O'Mera and Lease 1983)]

The advantage of the centrifuge method is speed; capillary pressures and relative permeability can be measured on three or six core samples simultaneously. An disadvantage is that the invading phase relative permeability can not be simultaneously measured

with accuracy and the invading phase relative permeability is measured by reversing the displacement. Fig. 5.20 compares relative permeability curves measured by the centrifuge compared with steady state measurements. These results were before the nonwetting phase model was implemented. Also, the steady state measurements were normalized with respect to the initial oil permeability.

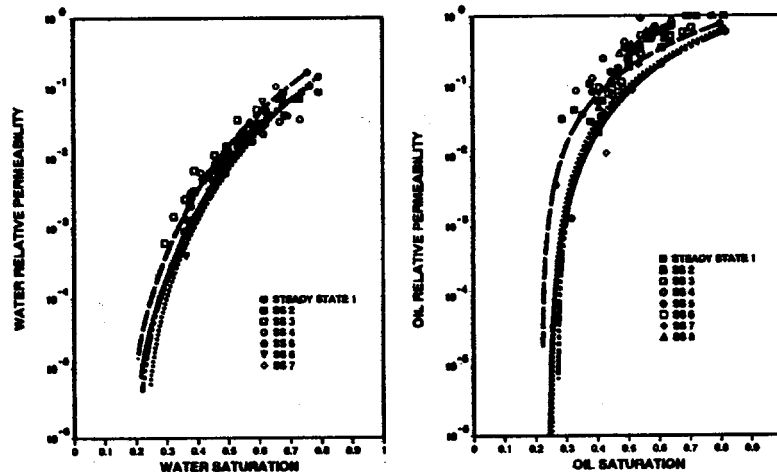


Fig. 5.20 Comparison of centrifuge (curves) and steady state (symbols) (Hirasaki, Rohan, Dudley 1992)

References

Anderson, W. G.: "Wettability literature Survey- Part 5: The Effects of Wettability on Relative Permeability", J. Pet. Tech. November, 1987, 1453-1987.

Baker, L. E.: "Three Phase Relative Permeability Correlations", SPE/DOE 17396, presented at the SPE/DOE Sixth Symposium on Enhanced Oil Recovery, 1988, Tulsa, OK.

Burdine, N. T.: "Relative Permeability Calculations from Pore Size Distribution Data", AIME Petroleum Trans., Vol. 198, (1953) 71-78.

Corey, A. T.: "The Interrelation Between Gas and Oil Relative Permeabilities", Producers Monthly, Nov. (1954), 38-41.

Hirasaki, G. J., Rohan, J. A., and Dudley, J. W. II: "Interpretation of Oil/Water Relative Permeabilities from Centrifuge Displacement", SPE 24879 paper presented at the 67 Annual Meeting of SPE (1992), Washington, D. C. Oct. 4-7.

Jadhunandan, P. P. and Morrow, N. R.: "Effect of Wettability on Waterflood Recovery for Crude Oil/Brine/Rock Systems", SPE 22597, paper presented at the 66th Annual Meeting of SPE, 1991, Dallas, TX, Oct. 6-9.

Lake, L. W.: Enhanced Oil Recovery, Prentice Hall, New Jersey, 1989.

Stegemeier, G. L.: "Mechanisms of Entrapment and Mobilization of Oil in Porous Media", in Improved oil Recovery by Surfactant and Polymer Flooding, Shah, D. O. and Schechter, R. S. ed., Academic Press, New York, 1977.